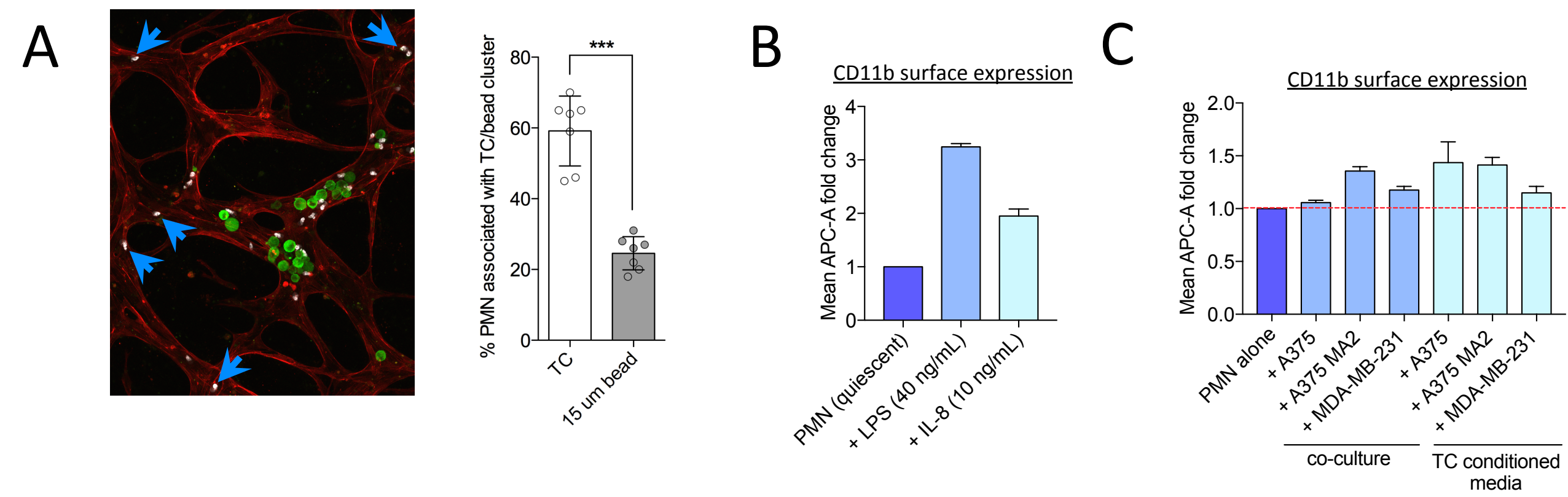
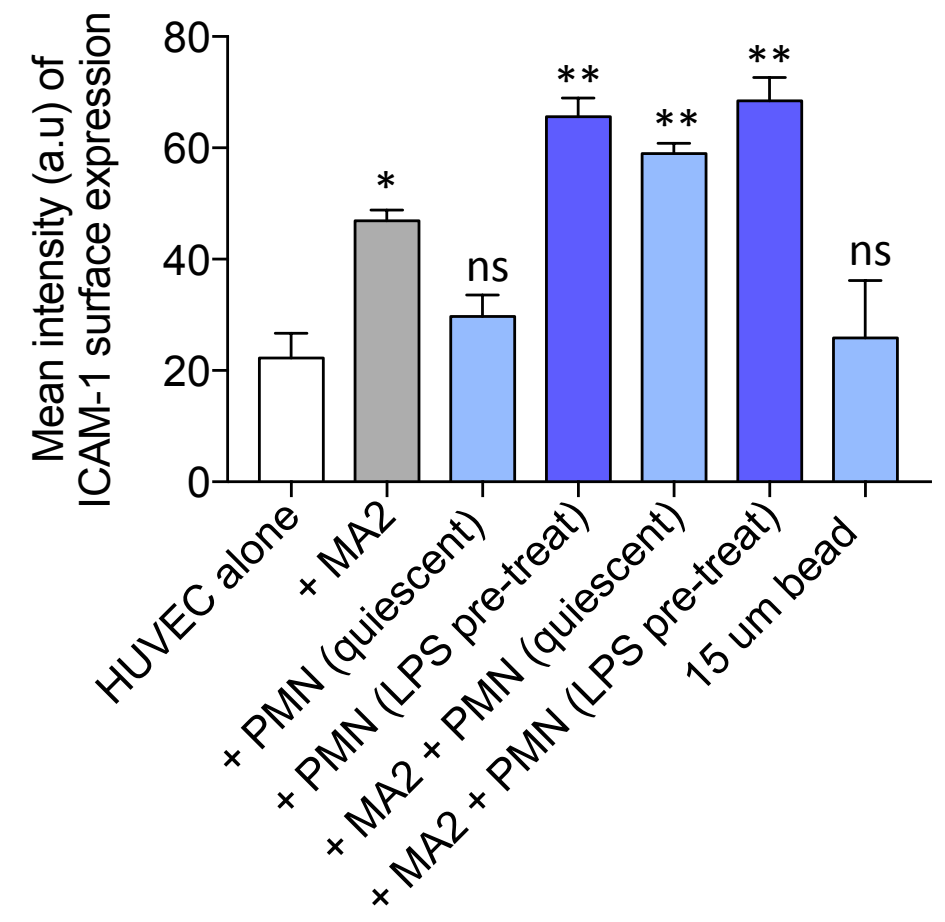
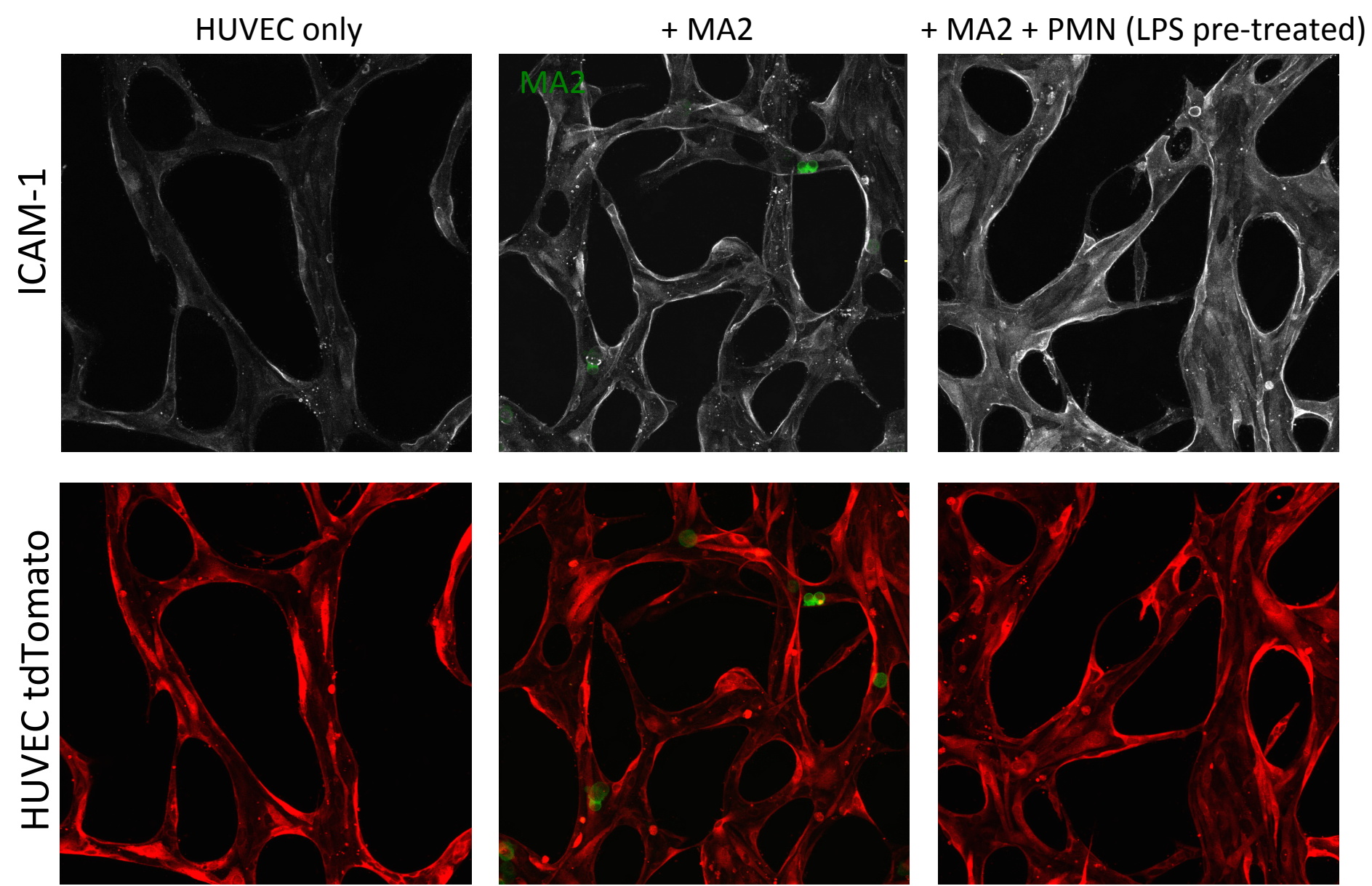


**Fig S1. (A)** Example photograph of a typical PDMS chip. **(B)** Top view schematic of chip design indicating the direction of fluid flow in the integrated reservoir (green) which results in orthogonal flow across micro-vessel beds controlled by the the ports and plugs layer (pink).

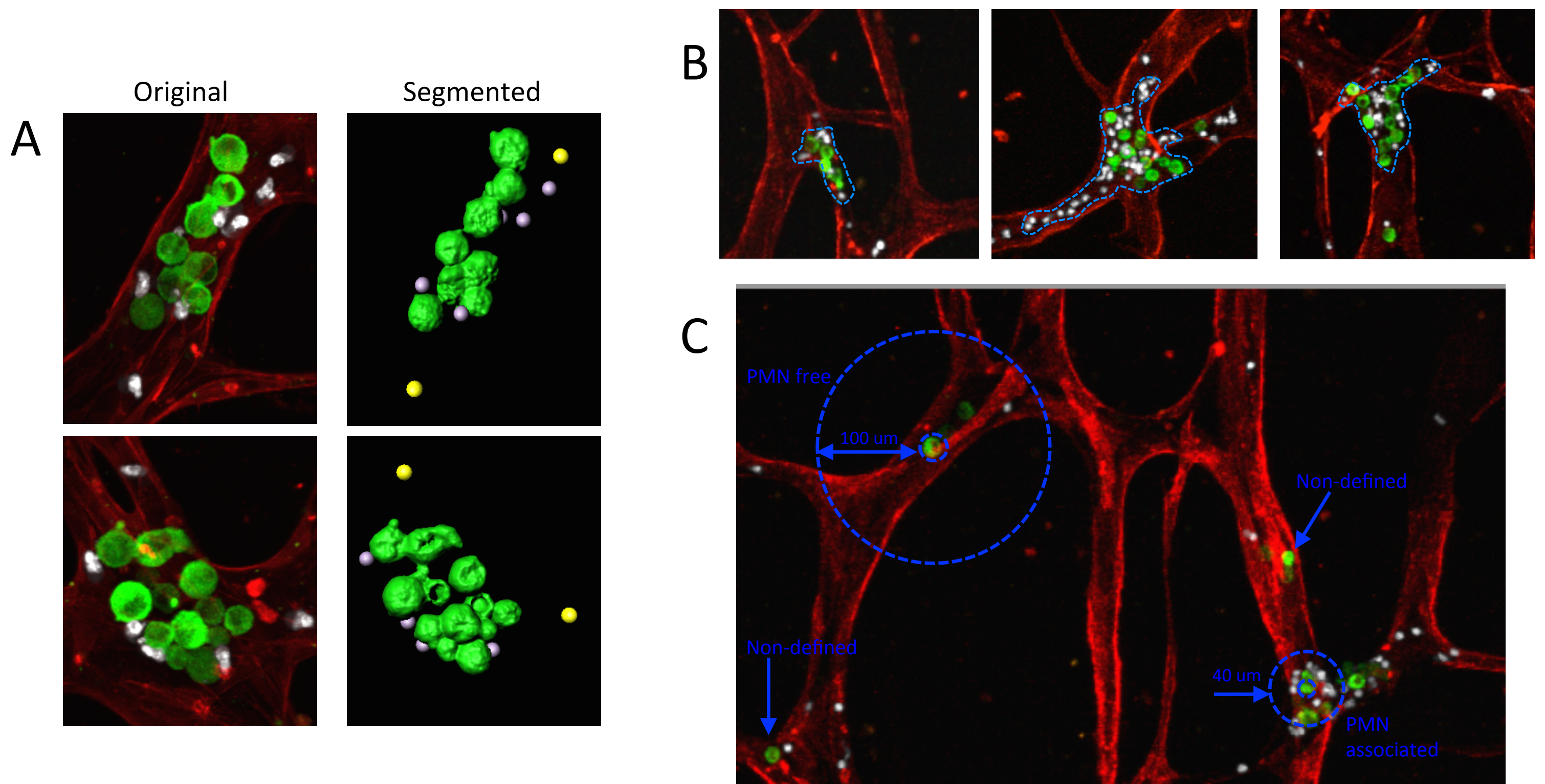


**Fig S2. (A)** Distribution of PMNs in microvascular bed association with TCs (blue arrows indicate PMNs that are not associated with TCs). Percentage of PMNs in a single device that is found to be clustered/associated with either tumor cells or 15 micron beads (each point represents one device). **(B)** Mean fold change from unstimulated PMNs in CD11b surface expression as determined by flow cytometry, when PMNs are treated with LPS or rhIL-8. **(C)** Mean fold change in CD11b surface expression when PMNS are co-cultured with A375, MA2-A375, MDA-MB-231 cells, or when incubated in the respective tumor conditioned media.



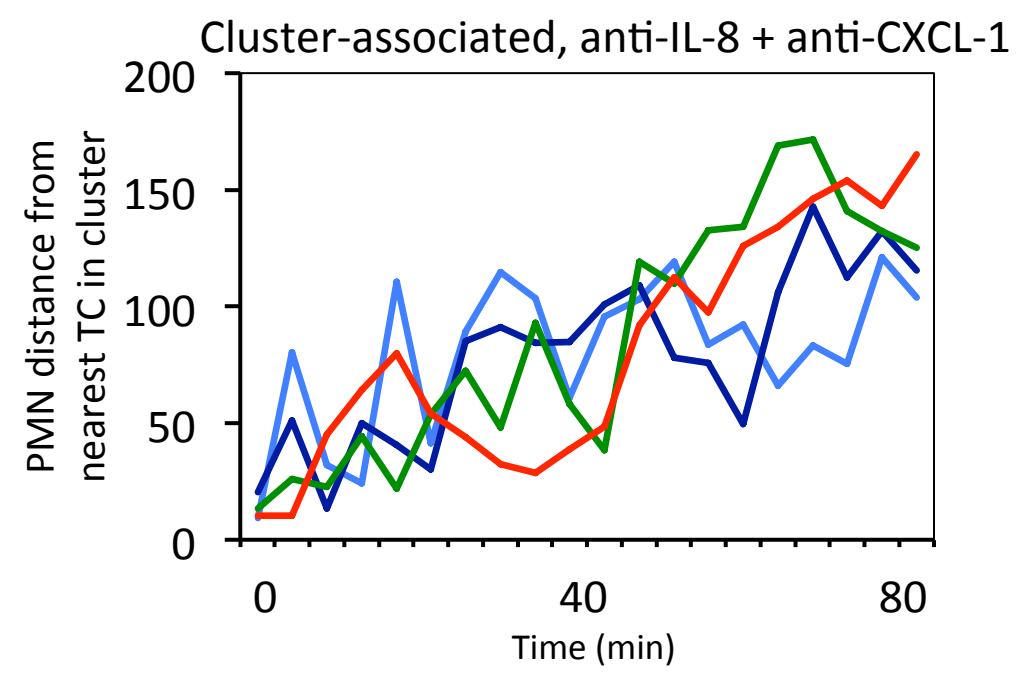
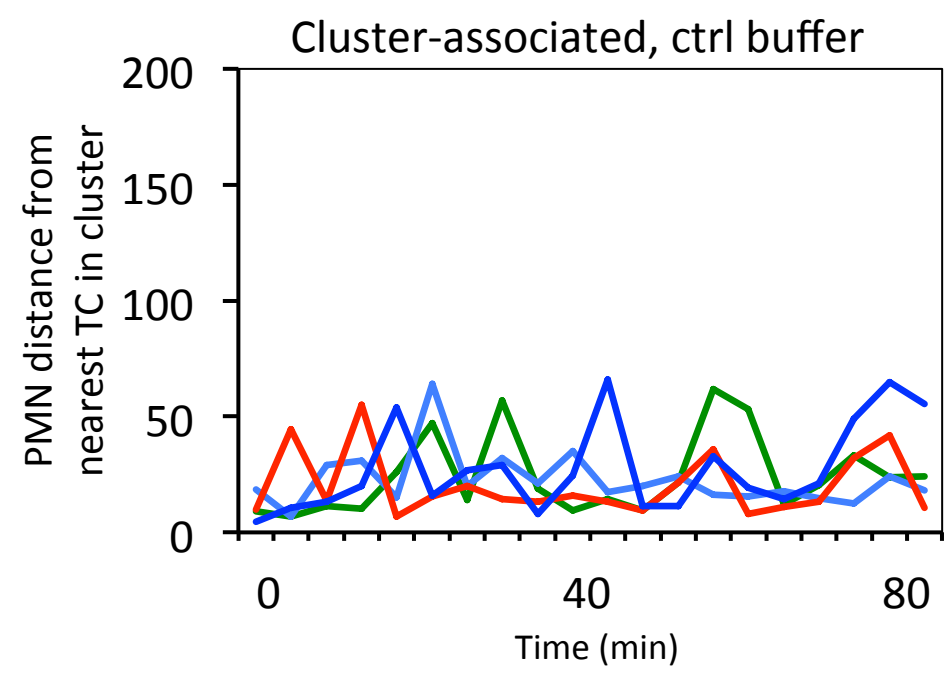
**SI Fig. 3.** Representative immunostaining images of ICAM-1 in unpermeabilized microvessels. Quantification of mean intensity of ICAM-1 signals normalized to area of vessel coverage (in arbitrary units).



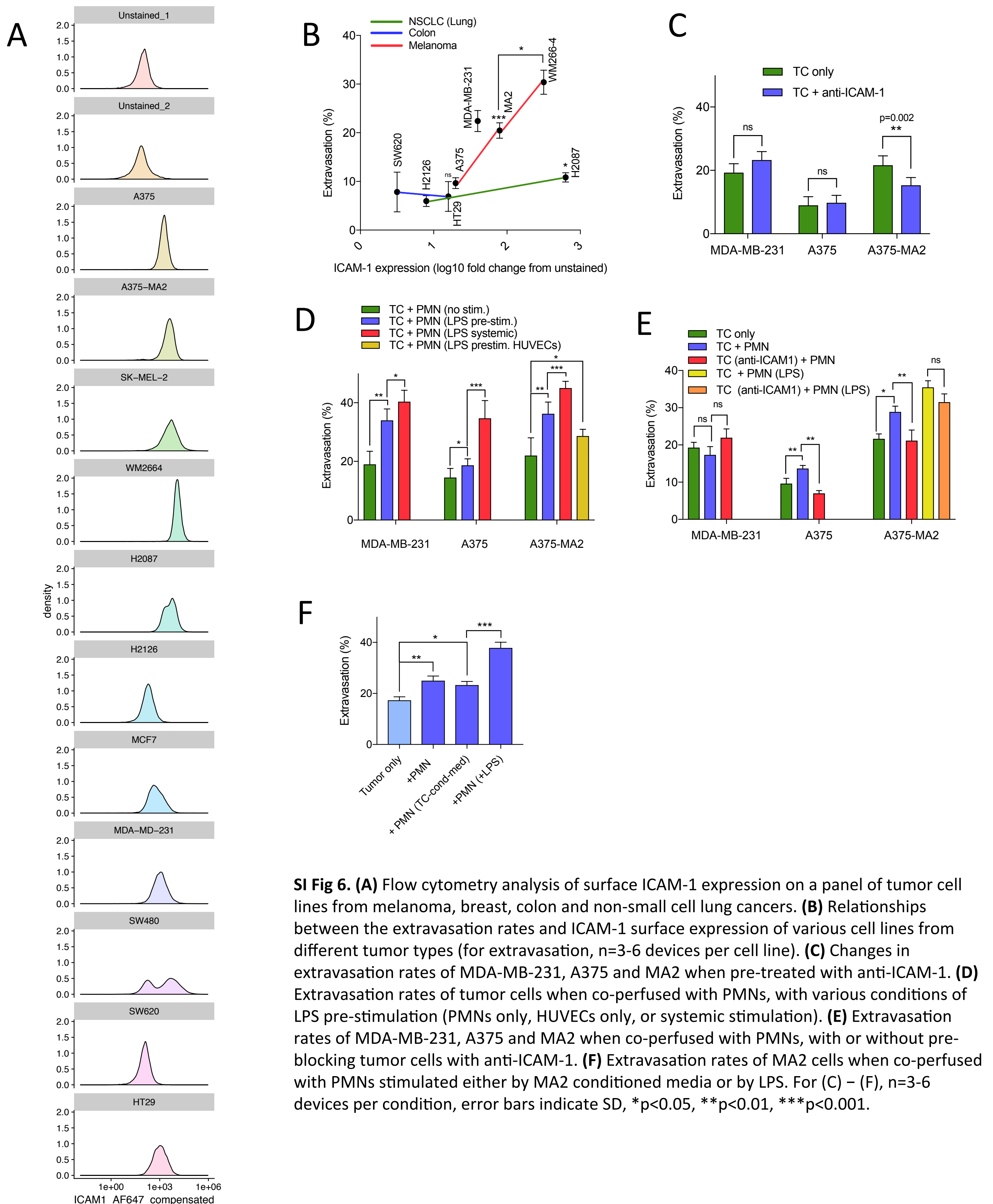


**Fig SI 4. (A)** Examples of original (maximum intensity projection) and segmented TCs and PMNs. PMNs are represented as 3 micron radius spheres. White spheres denote “cluster-associated” PMNs, while yellow spheres denote PMNs that are  $>10$  micron away from any other cells in the cluster, and hence are not part of the cluster (for definitions, see **Methods**). **(C)** Further examples of defined “TC-PMN clusters.” PMNs within the blue dotted boundary are classified as “cluster-associated” PMNs. PMNs that are not part of TC-PMN clusters and are at least 150  $\mu\text{m}$  away from any other clusters are defined as “free” PMNs. All other PMNs that do not satisfy either criteria are categorized as “undefined” to order to clearly discretize each population. **(D)** Examples of “PMN-associated” tumor cells and “free” tumor cells.

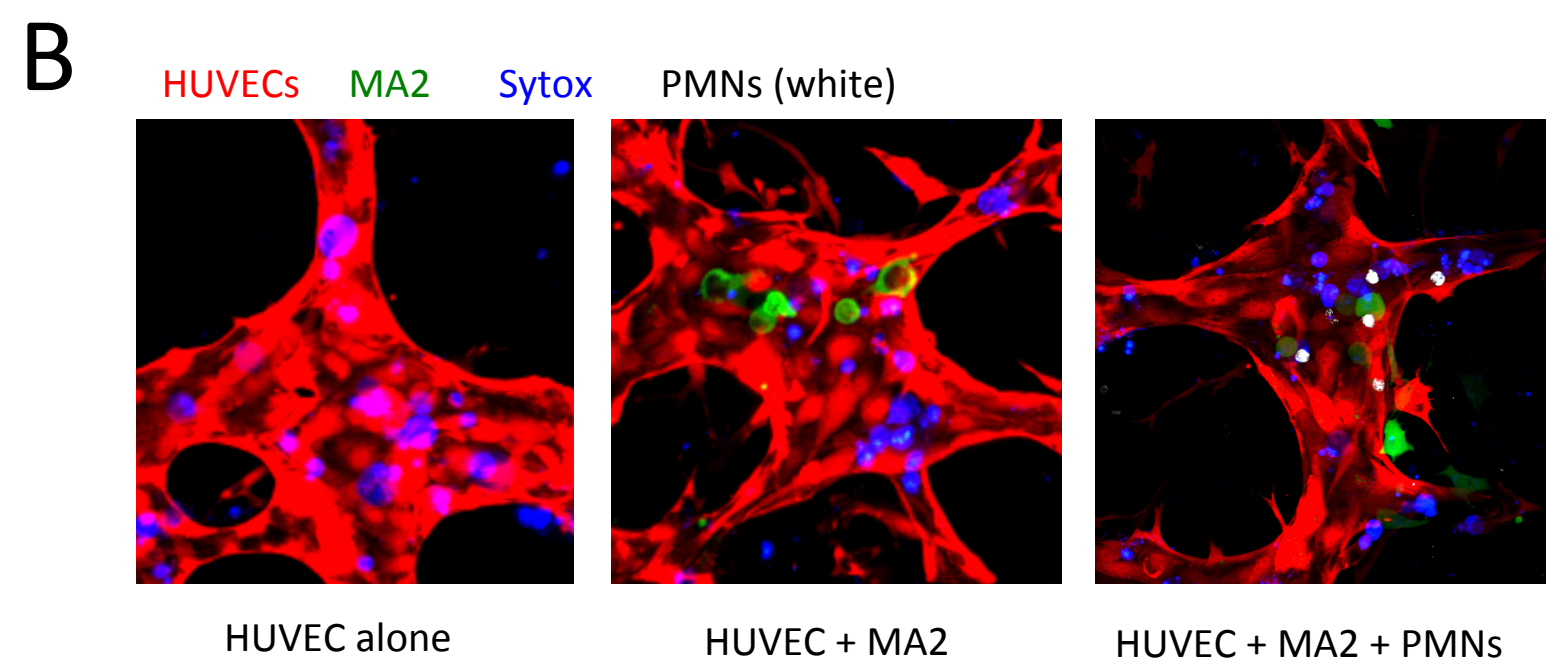
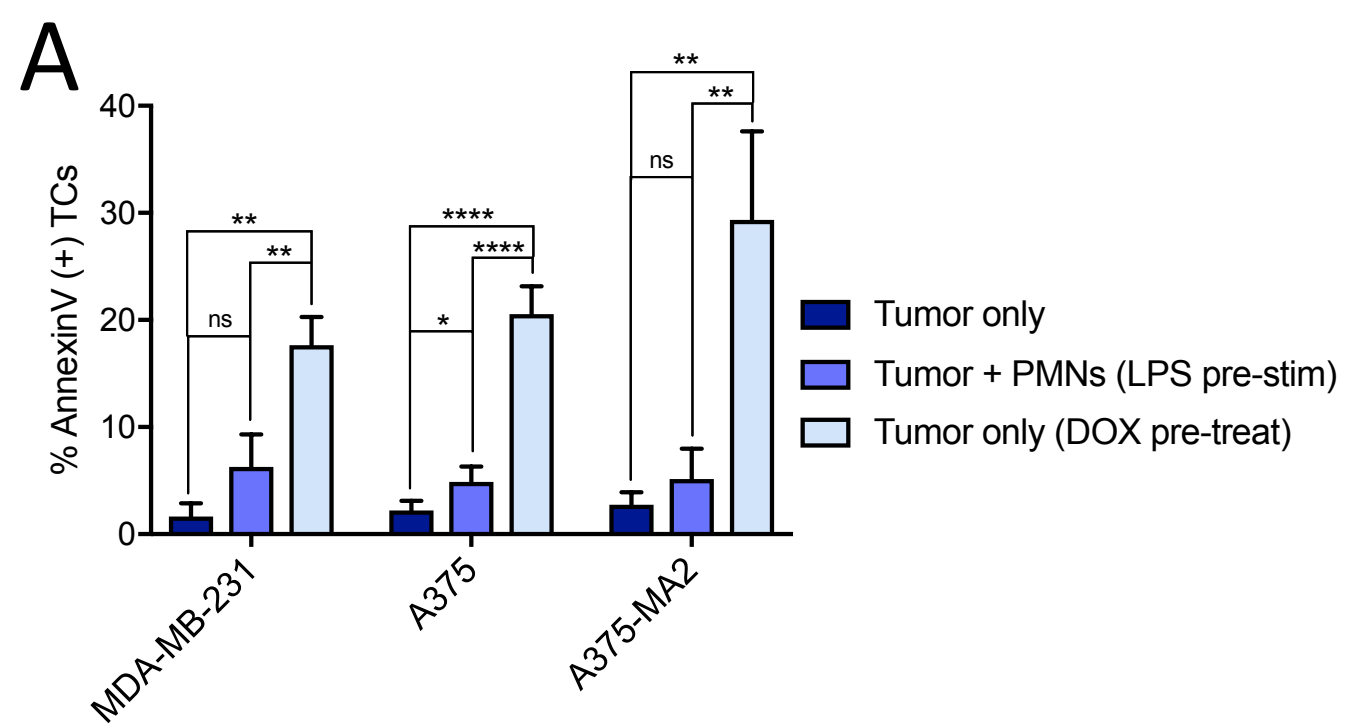




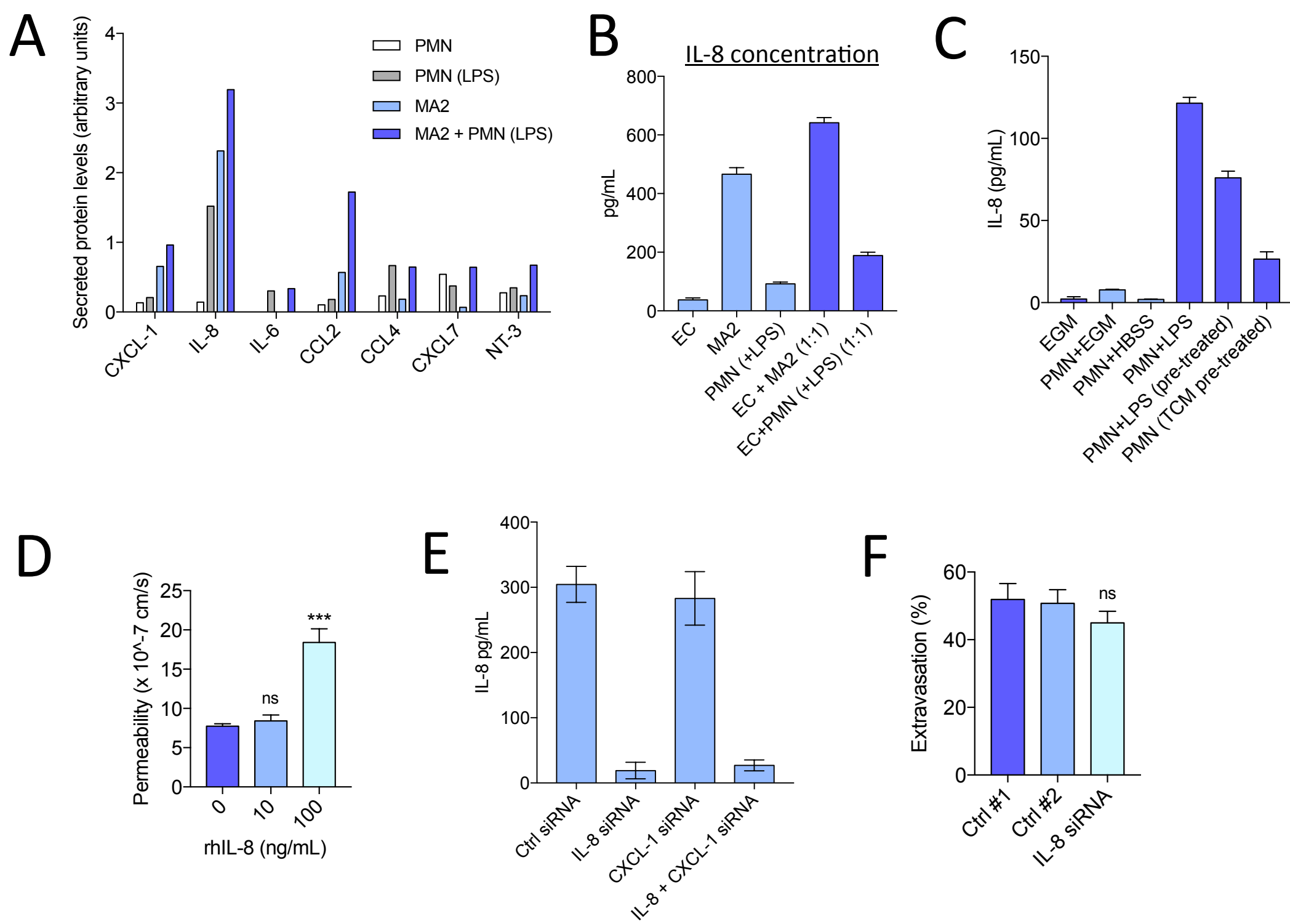
**Fig SI 5.** Quantification of the shortest distance of individual cluster-associated PMNs to the periphery of the TC-PMN cluster (drawn at  $t=0$ ). Four representative cluster-associated PMNs are shown for the case of control buffer **(A)** or anti-IL-8 + anti-CXCL-1 treatment **(B)**, which were analyzed at 4 minute intervals for 80 minutes.







**SI Fig 7. (A)** Quantification of AnnexinV staining on tumor cells in microvascular networks when tumor cells are alone, co-perfused with LPS-stimulated PMNs, or when tumor cells are pre-treated with Doxorubicin (positive control) (n=3-5 devices per condition). **(B)** Representative images of Sytox Green staining shows no apparent NET formation in the presence of LPS-stimulated neutrophils, compared to the controls (tumor only and HUVEC only). Blue=Sytox, red=HUVECs, green=MA2. Normal baseline levels of Sytox staining in the HUVEC only control shows staining of DNA from dead/dying cells trapped in the tissue (through the process of vessel formation over the course of 6 days).



**SI Fig 8. (A)** Relative levels of highest secreted cytokines from PMN, LPS stimulated PMNs, MA2 or MA2 + LPS stimulated PMNs in co-culture, as determined by a 80 human cytokine array. **(B)** Quantification of IL-8 secretion after 4 hours of adherent well plate culture. **(C)** Quantification of IL-8 secretion by PMNs when stimulated by varying conditions. **(D)** Permeability of micro vessels to 70kDa dextran after 4 hour treatment with 0, 10, or 100 ng/mL of recombinant human IL-8. **(E)** Quantification of IL-8 secretion by MA2s when treated with either IL-8 siRNA or CXCL-1 siRNA. **(F)** Extravasation rates of MA2 after treatment with Ctrl siRNA or IL-8 siRNA.



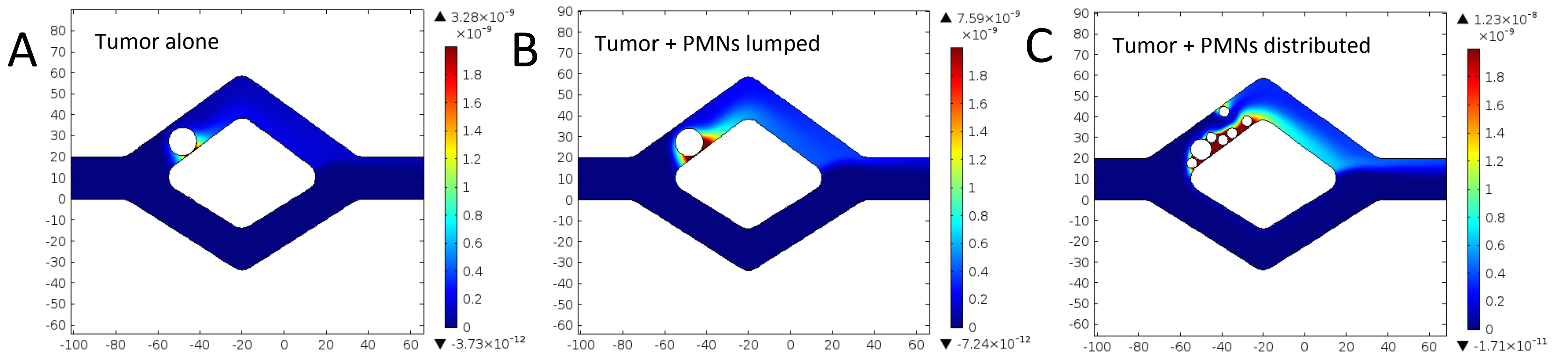


**Fig SI 9.** 2D maps of IL-8 concentrations (mol/m<sup>3</sup>) of intravascular IL-8 under physiological flow conditions, assuming constant flux of IL-8 from an arrested tumor cell, one tumor cell and 6 PMNs lumped in one source, or distributed.

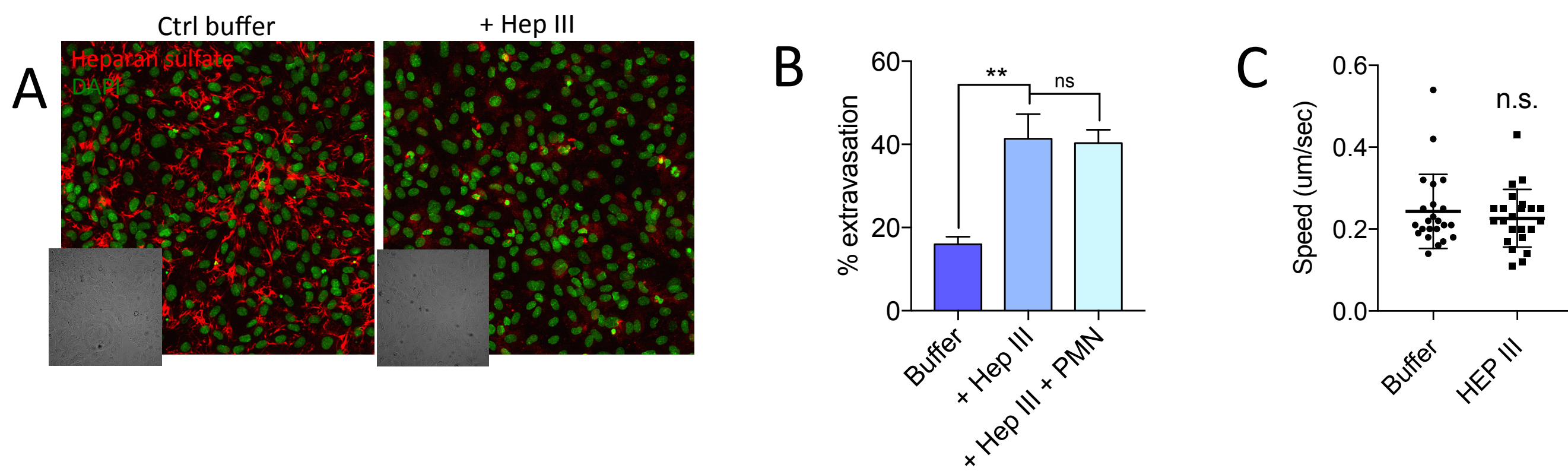
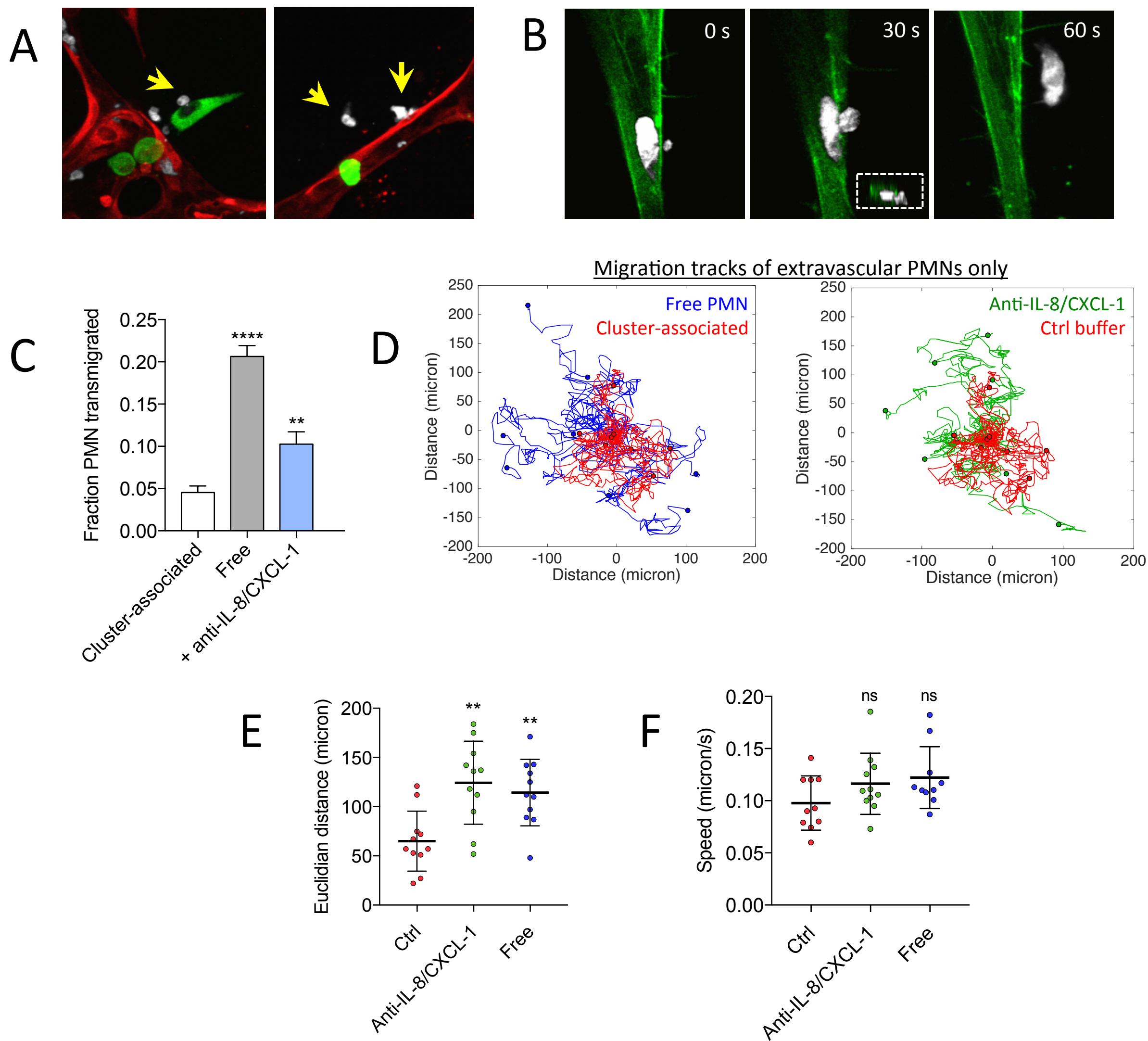


**Fig SI 10. (A)** Representative immunostaining (and phase – inset) of heparan sulfate (red) and nucleus (green) on the surface of HUVEC monolayers after 2 hours of treatment with 3U/mL of heparinase III. **(B)** Extravasation rates (at 6 hours) of MA2 alone or MA2 + stimulated PMNs without or without pre-treatment of microvascular heparinase III. **(C)** Migration speed of stimulated PMNs in microvasculature without or without pre-treatment with heparinase III.





**SI Fig 11. (A)** Representative images of both extravasated tumor cells (green) and extravasated PMNs (white) from within microvasculature (red). **(B)** Representative image of a typical transmigrating PMN from microvasculature occurring within 60 s. **(C)** Fraction of PMNs in each subpopulation (cluster-associated, free or associated with antibody treatment) which transmigrate into the extravascular matrix (at least once) over the span of 3 hours post seeding (n=4 devices/condition) **(D)** Migration tracks of extravascular PMNs that are cluster associated, free, or cluster associated and treated with anti-IL-8 and anti-CXCL-1 (8 representative PMN tracks plotted per condition). **(E)** Euclidian distance from original position of extravascular PMNs. **(F)** Migration speed of extravascular PMNs (n=9 cells per condition).

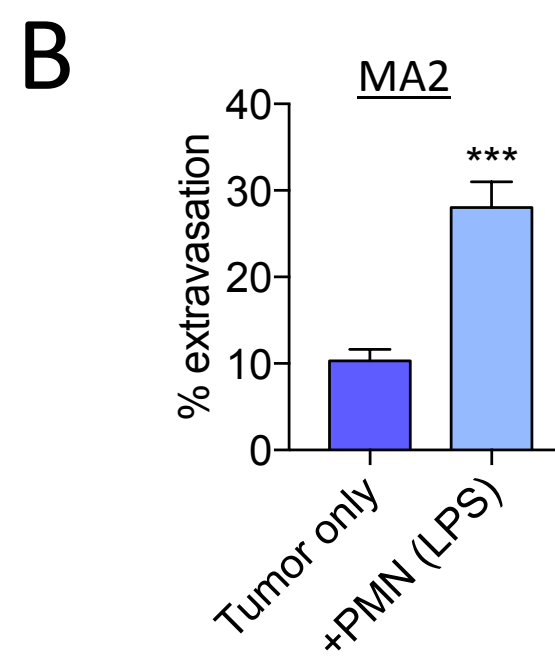
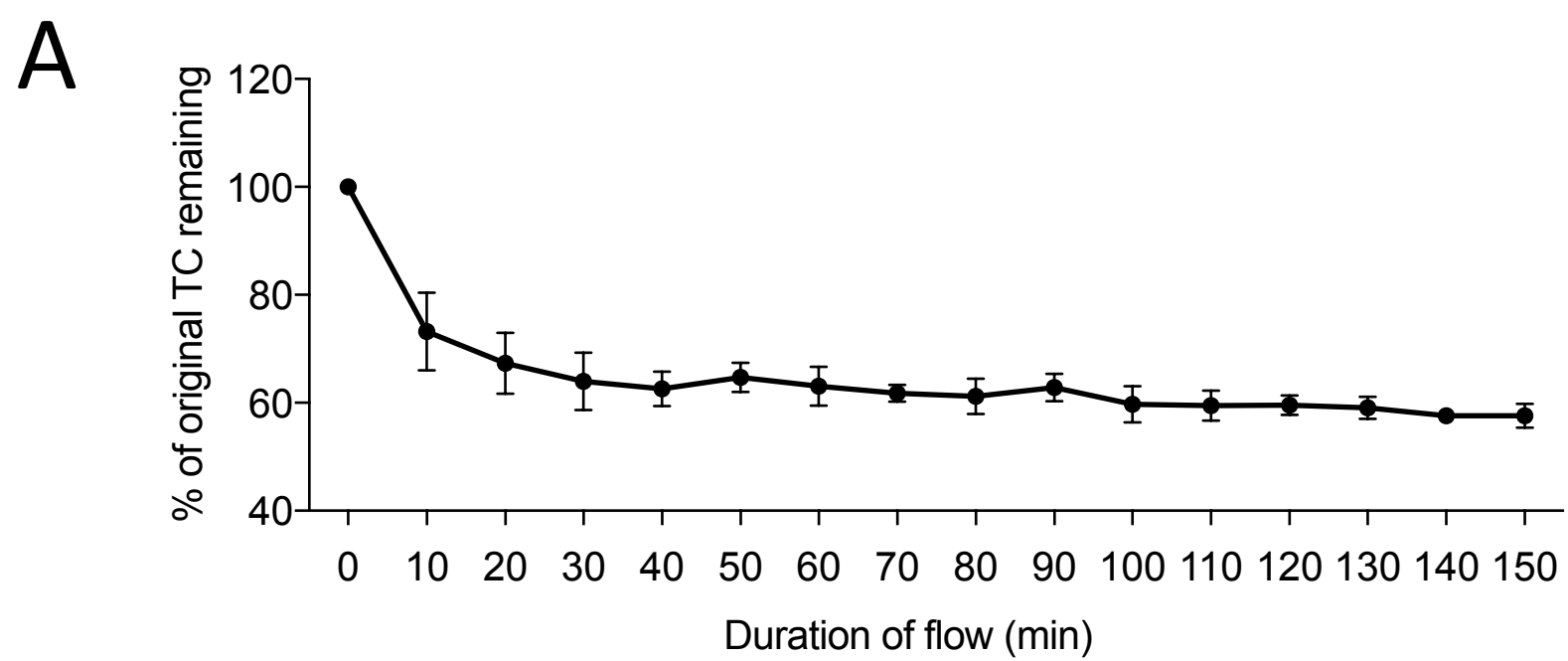


**Fig SI 12. (A)** Percentage of original number of trapped MA2 cells at t=0 remaining over the course of 150 minutes of microvascular bed perfusion. **(B)** Extravasation rates of MA2 alone or MA2 + LPS stimulated PMNs if rates were calculated as the number of extravasated cells at 6 hours divided by the number of cells at t=0 (instead of t=20 min). This definition effectively couples both effects of retention and transmigration caused by the addition of PMNs.



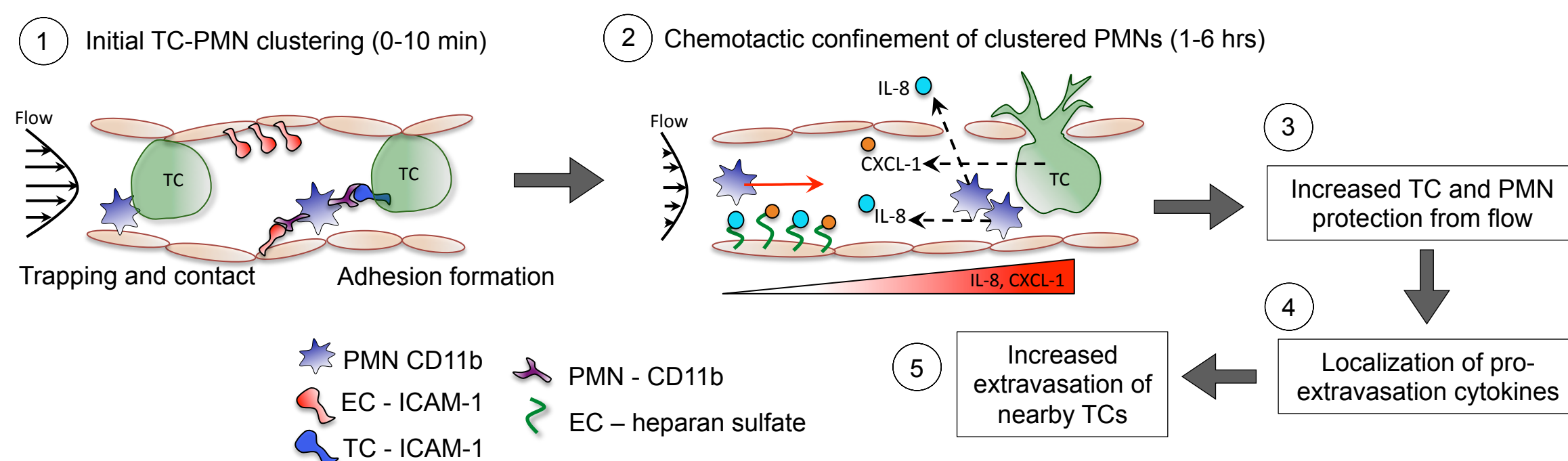


**Figure SI 13. PMN confinement at clusters enhances TC extravasation through spatial localization and sequestration of PMN-derived pro-extravasation factors at cluster-associated TCs.** Working hypothesis. (1) PMNs and TCs arrest in clusters under from physical trapping and engagement of CD-11b to EC-ICAM-1 and to TC-ICAM-1. (2) PMNs continue to be sequestered in clusters due to PMN-derived IL-8 and tumor derived CXCL-1. The chemotactic confinement of PMNs is enhanced by immobilization of chemokines within the EC glycocalyx. (3) The occlusion of vessels by PMN-TC clusters promotes cell retention by decreasing levels of flow entering the vessel segment. (4) Confinement of PMNs at clusters results in the spatial localization of pro-transmigration cytokines. (5) One of these factors is IL-8, which plays an additional role of enhancing extravasation potential of tumor cells, through the weakening of the endothelial barrier. Dotted arrows indicate chemokine secretion, red arrow indicates migration direction.

**Supplemental Table 1**

<b>Parameter</b>	<b>3D <i>in vitro</i> vascular networks with HUVECs and NHLFs</b>	<b><i>In vivo</i> measurements for mice lungs</b>
<b>Vessel diameter range</b>	7-110 $\mu$ m ([1])	7-120 $\mu$ m([2])
<b>Vessel permeability</b>	(8.92 $\pm$ 1.47) $\times 10^{-7}$ cm/s for 70kDa ([1], [3], [4])	7.1-12.4 $\times 10^{-7}$ cm/s for 70kDa measured via a dorsal skinfold chamber ([5])
<b>Flow velocity</b>	(2.71 $\pm$ 1.27) mm/s ([1])	(0.3681 $\pm$ 0.0141) mm/s in rat lung ([6])
<b>Shear stress on vessels</b>	~1 Pa ([1])	0.5-1 Pa (postcapillary venules to arteries) ([7])

References

- [1] M. B. Chen, J. A. Whisler, J. Fröse, C. Yu, Y. Shin, and R. D. Kamm, "On-chip human microvasculature assay for visualization and quantification of tumor cell extravasation dynamics," vol. 12, no. 5, pp. 865–880, 2017.
- [2] S. X. Vasquez, F. Gao, F. Su, V. Grijalva, J. Pope, B. Martin, J. Stinstra, M. Masner, N. Shah, D. M. Weinstein, R. Farias-Eisner, and S. T. Reddy, "Optimization of microCT imaging and blood vessel diameter quantitation of preclinical specimen vasculature with radiopaque polymer injection medium," *PLoS One*, vol. 6, no. 4, pp. 2–7, 2011.
- [3] M. B. Chen, J. A. Whisler, J. S. Jeon, and R. D. Kamm, "Mechanisms of tumor cell extravasation in an *in vitro* microvascular network platform," *Integr. Biol.*, vol. 5, no. 10, pp. 1262–1271, 2013.
- [4] J. a Whisler, M. B. Chen, and R. D. Kamm, "Control of perfusable microvascular network morphology using a multiculture microfluidic system.," *Tissue Eng. Part C. Methods*, vol. 20, no. 7, pp. 543–52, Jul. 2014.
- [5] M. R. Dreher, W. Liu, C. R. Michelich, M. W. Dewhirst, F. Yuan, and A. Chilkoti, "Tumor vascular permeability, accumulation, and penetration of macromolecular drug carriers," *J. Natl. Cancer Inst.*, vol. 98, no. 5, pp. 335–344, 2006.
- [6] G. Hanna, A. Fontanella, G. Palmer, S. Shan, D. R. Radloff, Y. Zhao, D. Irwin, K. Hamilton, A. Boico, C. A. Piantadosi, G. Blueschke, M. Dewhirst, T. McMahon, and T. Schroeder, "Automated measurement of blood flow velocity and direction and hemoglobin oxygen saturation in the rat lung using intravital microscopy," *AJP Lung Cell. Mol. Physiol.*, vol. 304, no. 2, pp. L86–L91, 2013.
- [7] S. Sheikh, G. E. Rainger, Z. Gale, M. Rahman, and G. B. Nash, "Exposure to fluid shear stress modulates the ability of endothelial cells to recruit neutrophils in response to tumor necrosis factor- $\alpha$ : a basis for local variations in vascular sensitivity to inflammation," vol. 102, no. 8, pp. 2828–2834, 2003.

## SI Movie Captions

**Movie S1.** Confocal slice movie of simulated neutrophils (white) migrating in a lumen within the on-chip microvascular bed (red). Images are taken every 12 s.

**Movie S2.** Inflamed PMNs at a TC-PMN cluster exhibiting dispersion migratory behavior (white = PMNs, green = MA2, red = HUVECs). Images taken every 35 s.

**Movie S3.** Inflamed PMNs at a TC-PMN cluster exhibiting confined migratory behavior (white = PMNs, green = MA2, red = HUVECs). Images taken every 35 s.

**Movie S4.** Migratory behavior of extravascular inflamed PMNs (white) near arrested tumor cell clusters (green). Images taken every 35 s.

**Movie S5.** Movie showing the flow and arrest of MA2 tumor cells (green) and human PMNs (white) within zebrafish embryo vasculature, imaged via confocal microscopy (projection of 50um z-stacks, time step = 14 s)

**Movie S6.** Confocal projection of one region of interest depicting the migratory nature of PMNs (white) within *in vitro* human vasculature (red). Images taken every 8 min.

**Movie S7.** Example of 1 micron polystyrene beads flowing through a representative *in vitro* vascular bed (real-time) under a 4 mm H<sub>2</sub>O hydrostatic pressure drop.

**Movie S8.** Example of 1 micron polystyrene beads co-perfused with MA2 tumor cells, flowing through a representative region in a *in vitro* vascular bed (real-time) under a 4 mm H<sub>2</sub>O hydrostatic pressure drop.



## **Supplementary Methods**

### **Cell culture and treatments**

Pooled human umbilical vein ECs (HUVECs) (Lonza) were transduced with a mCherry LifeAct plasmid (Addgene), and cultured in EGM-2MV supplemented with Singlequots™ (Lonza, Walkersville) on collagen-1 coated plates and used at passage <6. Normal human lung fibroblasts (Lonza) were cultured in FGM-3 supplemented with Singlequots™ (Lonza, Walkersville) and used at passage <12. Human GFP expressing melanoma A-375 and A-375 MA2 (gift from the Hynes Lab, MIT) and MDA-MB-231 (ATCC) were maintained in DMEM supplemented with 10% FBS and 1% penicillin/streptomycin. For tumor cell and PMN perfusion, cells were trypsinized and resuspended at  $1.2 \times 10^6$ /mL and mixed with PMNs to achieve a final density of  $0.6 \times 10^6$  /mL (tumor) and  $3 \times 10^6$ /mL (PMN). Subsequently, 50  $\mu$ L of the mixed cell suspension were injected into each device.

### **Device design and fabrication**

The microfluidic chip used this study is an improved version of our previous design<sup>20</sup>. Briefly, we employed wider channels (500  $\mu$ m wide by 130  $\mu$ m high) in the branching network leading to the entrance of each gel region, combined with a narrow channel (120  $\mu$ m wide) downstream of the gel region prevents premature leakage of hydrogel into the side channels if any other is prematurely filled. Since fibrinogen polymerizes rapidly once in contact with thrombin, the branching network length and channel width were designed to reduce the tendency for premature polymerization before all 8 devices have been filled. Although the gel regions are all connected via the same branching network, they can be considered to be independent since the characteristic diffusion time scale is on the order of days for small proteins in water ( $D \sim 10^{-6}$  cm<sup>2</sup>/s). This is negligible compared to the time span of a typical extravasation experiment in our assay (8-12 hours).

Constant media perfusion is achieved via a ~5 mm passive hydrostatic pressure head using a large integrated reservoir attached to the top of the device after introduction of the tumor cells into each microvascular bed (**Fig. 1b**). The reservoir and channels are separated by a dual-purpose “ports and plugs” layer, which simultaneously provides access to and restricts flow in a manner that allows formation of identical

pressure drops across all 8 regions in the direction orthogonal to that in the reservoir. Using this simple pump-free method, physiologically relevant shear stresses on the order of ~1 Pa can be robustly maintained for ~ 6 hours before significant changes (>10%) in the pressure drop occur. In cases where the experiment was longer, fluid was replenished in reservoirs to restore the original hydrostatic pressure drop, and the reservoir was carefully secured to the chip using C-clamps to prevent delamination over time.

In addition, the larger gel-cell mixing volume decreases variations in cell densities between hydrogel regions in one entire chip, which is critical for improving the percentage of perfusable vascular beds in each experiment. Furthermore, with no changes to the volume of perfusable networks and the number of starting HUVECs and FBs, the number of independent devices that can be filled in one experiment is increased at least 4-fold (>56). This is partly due to the significant reduction in the dead-volume by replacing 8 gel injection ports with one, while parallel seeding significantly reduces the time required to seed a single hydrogel region independently.

Preparation of cells for device injection is similar to that described previously<sup>21</sup> with some modifications. Briefly, HUVECs were resuspended in a thrombin solution (1U/mL in EGM-2MV) at  $13 \times 10^6$ /mL and mixed in a 1:1 ratio with fibrinogen solution (6 mg/mL) (Sigma) by pipetting exactly 4 times, to create a final volume of 50  $\mu$ L. The mixed solution was immediately injected into the microchip via the injection port until all 8 chambers have been filled. Similarly, NHLFs were resuspended to a concentration of  $4 \times 10^6$ /mL and injected in the same manner on the opposite side. After 15 min of polymerization in humidified chambers at RT, EGM-2MV was injected into all media channels and devices were cultured at 37°C and 5% CO<sub>2</sub> for 4 days prior to vessel perfusion with tumor cells or 15  $\mu$ m fluorescent polystyrene beads (Invitrogen). Media was replenished every 24 h.

### **Cytokine array**

MA2 were plated onto 6 well plates in EGM-2MV until 60% confluence, after which media was replaced and incubated for 4 hrs before collection conditioned media. In some cases, freshly isolated PMNs were also incubated on 6 well plates, or co-incubated with MA2 cells, for 4 hrs in EGM-2MV. Conditioned media was centrifuged at 800g for 10 min to remove debris and stored at -20°C until use. Undiluted conditioned

media and EGM-2MV control media was assayed using a human 80-cytokine array (Cat #. AAH-CYT-5, Raybiotech), following the manufacturer's protocol.

### **Antibodies and reagents**

For blocking of neutrophil surface CD11b after LPS activation, cells were incubated with anti-CD11b (1:200 in HBSS) (Cat #. 101213, Biolegend) for 30 min at 4°C, followed by an HBSS wash. Tumor ICAM-1 was blocked by a 30-min incubation with anti-ICAM-1 diluted 1:200 in DMEM (Cat #. BBA9, R&D) at 4°C. HUVEC ICAM-1 was blocked by perfusing vascular networks with anti-ICAM-1 (1:200 in EGM-2MV) and devices were incubated for 30 min at 37°C followed by 2 washes with EGM-2MV before perfusion of cells. At times, HUVEC microvessels were stimulated with recombinant human IL-8 (Cat #. 208-IL, R&D) diluted at various concentrations in EGM-2MV for 3 hrs at 37°C prior to cell perfusion. To degrade the endothelial heparan sulfate layer, microvascular networks were pre-incubated with heparinase III from flavobacterium heparinum (Cat #. H88891, Sigma) at 3U/mL for 2 hrs prior to tumor cell perfusion. At times, HUVEC vessels were pre-treated with undiluted conditioned media (collected as described above) from tumor cells or PMNs for 3 hrs prior to cell perfusion with the same media.

To test the influences of various cytokines on PMN dispersion and TC extravasation, tumor cells mixed with LPS activated PMNs (at final perfusion densities) were incubated with anti-CXCL at 15 µg/mL (Cat #. MAB275), anti-IL-8 at 1 µg/mL (Cat #. MAB208), anti-CCL-4 at 5 µg/mL (Cat #. MAB271), anti-CXCL-7 at 20 µg/mL (Cat #. MAB393), anti-IL-6 at 0.2 µg/mL (Cat #. MAB206), or control isotypes, all from R&D. Cells suspension were incubated with antibodies for 20 min on ice followed immediately by perfusion into microvascular networks (without washing).

For siRNA mediated knockdown of IL-8 and CXCL-1 in MA2, cells were plated on six well plates and transfected with 25 pmol of IL-8 (Cat #. s7327) and/or CXCL-1 (Cat #. 215133) Silencer Select siRNA (Thermo Fischer) using Lipofectamine RNAiMax reagent (Thermo Fischer) (treated twice over 48 hrs), before trypsinization and perfusion into microvessels. Knockdown on secreted proteins was confirmed via ELISA (Cat #. D8000C, R&D).

For NET visualization, devices were incubated for 30 minutes at 37°C with SYTOX Orange Nucleic Acid Stain (Cat #. S11368) at 5µM in Vasculife (LL-0003) by



applying a hydrostatic pressure drop across the gel channel. Devices were immediately imaged following staining.

Early signs of apoptosis were detected in tumor cells by incubating the fixed devices with anti-AnnexinV (1:200) (Cat #. ab14196) overnight at 4C in blocking buffer. For positive controls, tumor cells were incubated at 37°C with doxorubicin diluted at 1.5µg/mL in DMEM (Cat #. sc-280681) for 24 hours, washed once with PBS and perfused into the microvascular networks.

### **Immunostaining**

Microfluidic chips were fixed with 4% paraformaldehyde for 10 min, not permeabilized (to stain for cell surface proteins only), and blocked with 3% BSA and 10% normal goat serum in PBS for 5 h. Samples were then incubated in primary antibodies against active conformation of CD11b (1:200) (Cat #. 301407, Biolegend), ICAM-1 (1:100) (Cat #. 353104, Biolegend), and heparan sulfate (1:100) (Cat #. 370255-S, Amsbio) overnight at 4C in blocking buffer. Devices were washed with PBS for 5 hrs and incubated with secondary antibody (Alexa Fluor 647 or Alexa Fluor 568, Invitrogen) at 1:200 for 4 hrs.

### **Zebrafish embryo extravasation assay**

The *casper* (*roy*<sup>-/-</sup>;*nacre*<sup>-/-</sup>) line was a kind gift from Dr. Leonard Zon (Children's Hospital). The *flk:dsRed2* line (originally developed by Dr. Kenneth Poss (Duke)) was a kind gift from Dr. Mehmet Yanik (MIT). The *flk:dsRed2* line was then crossed into the *casper* background. Embryos were 48 hours old when injected. One day before injection, embryos were dechorionated by adding 12 µL of 30 mg/mL pronase (Sigma) to each 10 cm plate containing embryos and incubating overnight.

Prior to injections, embryos were anesthetized in 0.02% tricaine (Sigma) buffered to pH 7.4 in aquarium make up water (AMW). Anesthetized embryos were then transferred to a 10 cm dish half-filled with 2% agarose and excess water was removed. Embryos were injected with 4 nL of 4x10<sup>4</sup> tumor cells per µL in PBS or 4x10<sup>4</sup> tumor cells and 2x10<sup>5</sup> human LPS-pre-stimulated PMNs per µL in PBS. Tumor cells and neutrophils were mixed together immediately prior to injections. The cells were injected

into the Duct of Cuvier just before it enters the heart. Embryos were maintained at 34°C following injection.

Injections were performed with borosilicate glass capillary needles (Warner Instruments) that were siliconized using sigmacote reagent (Sigma). Needles were pulled using a P-87 micropipette puller (Sutter Instrument) with the following settings: heat=800, pull=150, vel =150, time=200 and pressure=600. The tip of the needle was broken such that it dispensed 2 nL drops using a PLI-90A Pico-Liter Injector (Warner Instruments) set to an injection pressure of 2.0 PSI and an injection time of 0.10 seconds.

For time-lapse imaging, embryos were placed in a single well of a 6 well, glass-bottomed plate (MatTek) containing a thin layer of 2% agarose. They were then covered in 0.8% agarose containing 0.01% tricaine buffered to pH 7.4. Once the agarose solidified, the well was filled with AMW containing 0.01% tricaine buffered to pH 7.4.

For time point imaging, each well of a 96 well glass-bottom plate (MatTek) was filled with 60  $\mu$  L of 2% agarose. A previously described pin tool<sup>36</sup> was inserted into the wells for 20 min to generate agarose molds to orient embryos laterally for imaging. At the given time points, embryos were anesthetized in 0.01% tricaine in AMW buffered to pH 7.4 and added to each well.

Embryos were imaged on an A1R inverted confocal microscope (Nikon) using the resonant scanner with a 10x objective and 1.5x zoom. For time-lapse imaging, Z-stacks of 50  $\mu$  m with a 7.6  $\mu$  m step size were acquired every 14 seconds for 3 hrs. Fish were imaged within 6 hrs of injection. For time point imaging, a single 100  $\mu$  m Z-stack with a 7.6  $\mu$  m step size was acquired for each fish.

### **Confocal and epifluorescent time-lapse imaging**

Devices were imaged with a laser scanning confocal microscope (Olympus FV-1000) at 10X (N.A. 0.75) at 4-micron z-steps with 800X800 pixel resolution, every 20 min. For epifluorescent time lapses (Carl Zeiss), devices were imaged at 10X every 40-50 seconds. In both set-ups, devices were maintained at 37°C and 5%CO<sub>2</sub> for the duration of the time lapse. Time-lapse sequences were analyzed via Imaris Bitplane (for 3D confocal projections) and ImageJ (for 2D epifluorescent images).

### **Quantification of tumor cell or PMN extravasation**

In all experiments quantifying extravasation in microvascular networks, the transmigration rate of one device is calculated from 6 random fields of view via confocal microscopy at 20X (N.A. 0.75) with 1.26-micron z-steps and 800 X 800 pixel size. 3D projections were reconstructed in Imaris Bitplane. All tumor cells or PMNs that were observed to partially cross or completely clear the endothelial barrier were classified as “extravasated.” In order to de-couple the effects of PMNs on TC retention and the potential ability of PMNs to directly modulate transendothelial migration, extravasation rates were determined as the number of transmigrated cells divided by the number retained after 30 min of flow (after which tumor cell retention rates begin to plateau) (**SI Fig. 3c**).

### **Image segmentation, determination of TC-PMN clusters, cluster-associated or free PMNs/TCs**

Because TC-PMN clusters are heterogeneous in cell numbers, area coverage, cell-cell ratios, and cell-cell separation distances, we defined a “TC-PMN cluster” as any aggregate of cells with at least 1 tumor cell and 6 PMNs, each of which must be no more than 10  $\mu\text{m}$  away from nearest cell in the cluster (determined from images at  $t=0$ ). Relative distances between all cells were determined beforehand by segmentation of TCs into surfaces (thresholded) and PMNs (into 3  $\mu\text{m}$  radius spots), using the “Surfaces” and “Spots” functions, followed by the “Distance Transformation” function on Imaris Bitplane. Furthermore, the cluster must be at least 150  $\mu\text{m}$  away from other defined clusters (see **Supplementary Fig. 4a-b** for examples). PMNs lying within TC-PMN clusters were categorized as “cluster-associated,” while those free from clusters and within a 150  $\mu\text{m}$  radius of the cluster boundary were classified as “free.” Approximately 60% of PMNs arrested in a device are classified as “cluster-associated” and ~25% as “free” while the ones not clearly fitting either category (~15%) were “undefined.”

To determine the fractions of PMNs remaining over time, the periphery of each TC-PMN cluster defined at  $t=0$  was delineated by generating a minimum bounding sphere around the cluster, using Image J. At each 20-min time frame cells that remained within a 50  $\mu\text{m}$  radius from the defined periphery were considered to be “remaining,” while those outside of the 50  $\mu\text{m}$  radius was deemed “lost.” The fraction remaining was determined by taking the fraction of the total PMNs remaining over the 5 analyzed clusters in one device. The mean of at least 5 devices per condition is presented.

Conversely, to categorize “PMN-associated” TCs or “PMN-free” TCs, a similar metric was applied. If a tumor cell has at least 6 PMNs within a 40  $\mu\text{m}$  radius from the tumor cell periphery, it was categorized as “PMN-associated.” If the tumor cell has less than 2 PMNs within a 100  $\mu\text{m}$  radius is deemed “PMN-free.” Tumor cells do not fall into either category is “undefined” and not used for this specific analysis (see **Supplementary Fig. 4c** for examples). The extravasation rate of each subpopulation is determined by taking the fraction of the total number of PMN-associated TCs or free-TCs extravasated in a single device, and the average of at least 5 devices is presented.

### **Tracking of PMN migration**

To determine migration tracks of PMNs, epifluorescent images taken every 40-50 s were segmented (via ImageJ) to clearly delineate individual PMNs. PMNs were manually tracked using the “Manual Tracking” algorithm and paths were plotted using MATLAB.

To determine the migration speeds and euclidian distances of cluster-associated PMNs or free PMNs, representative cells were randomly chosen based and their categorization was based on their position at the first time point of imaging (“t=0”), despite the fact that their association with clusters may change over time. Each point represents one PMN, and statistics are determined by averaging speeds of analyzed PMNs in one device, with n=5 devices per condition.

### **Human neutrophil isolation**

Briefly, blood anti-coagulated with sodium citrate was layered onto Histopaque 1077 (Sigma), centrifuged (without brake at 1400 rpm), and plasma and PMBC layers were removed. PMNs were further separated using a density gradient with 2% dextran (Sigma) for 30 min at 1400 rpm, followed by red blood cell lysis with cold water. All procedures were done at room temperature. Isolated cells were resuspended at  $6 \times 10^6/\text{mL}$  in HBSS and stained with Cell Tracker Deep Red<sup>TM</sup> (Invitrogen) at 0.5  $\mu\text{M}$  for 10 min and washed twice with HBSS. In experiments requiring inflamed PMNs, cells were further incubated with 30 ng/mL of LPS (Sigma) for 25 min at 37°C, and washed 3 times with HBSS.